Poly(ADP-ribose)polymerase activates Mre11 at stalled replication forks to promote replication restart and homologous recombination

Helen E. Bryant, Eva Petermann, Niklas Schultz, Ann-Sofie Jemth, Olga Loseva, Natalia Issaeva, Fredrik Johansson, Serena Fernandez, Peter McGlynn and Thomas Helleday

Supporting Figures

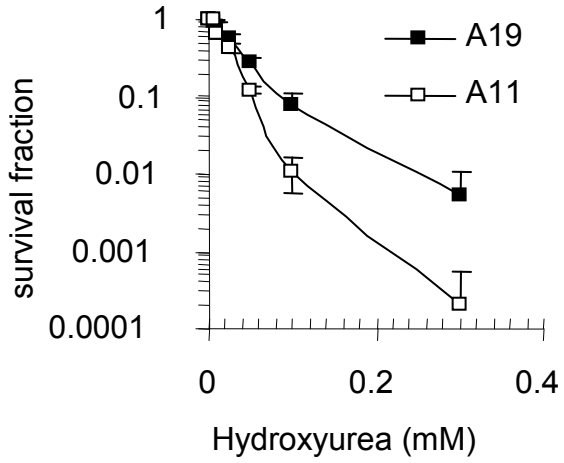

Figure S1 Absence or inhibition of PARP1 leads to increased sensitivity to hydroxyurea. Survival fraction of A19 (PARP1+/+) and A11 (PARP1-/-) MEFs following treatment for 10 days with increasing doses of the replication inhibitor hydroxyurea. The means (symbol) and standard deviations (error bar) from at least three experiments are depicted.

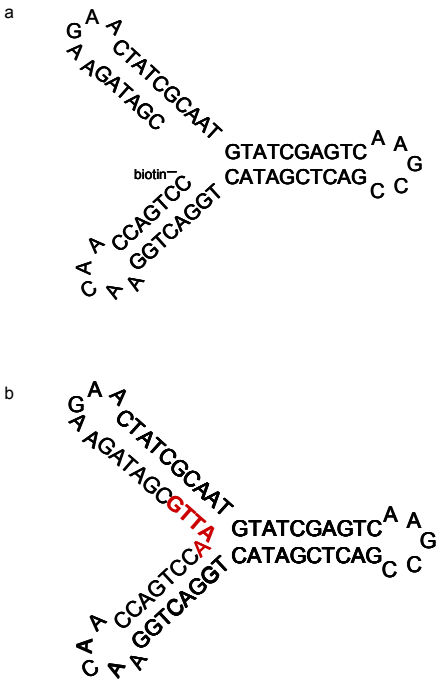

Figure S2 Predicted molecular structure of (a) biotin labelled stalled fork construct and (b) ligated stalled fork construct. A hairpin was included in the artificial constructs as it has been reported earlier that PARP1 binds efficiently to DNA ends.

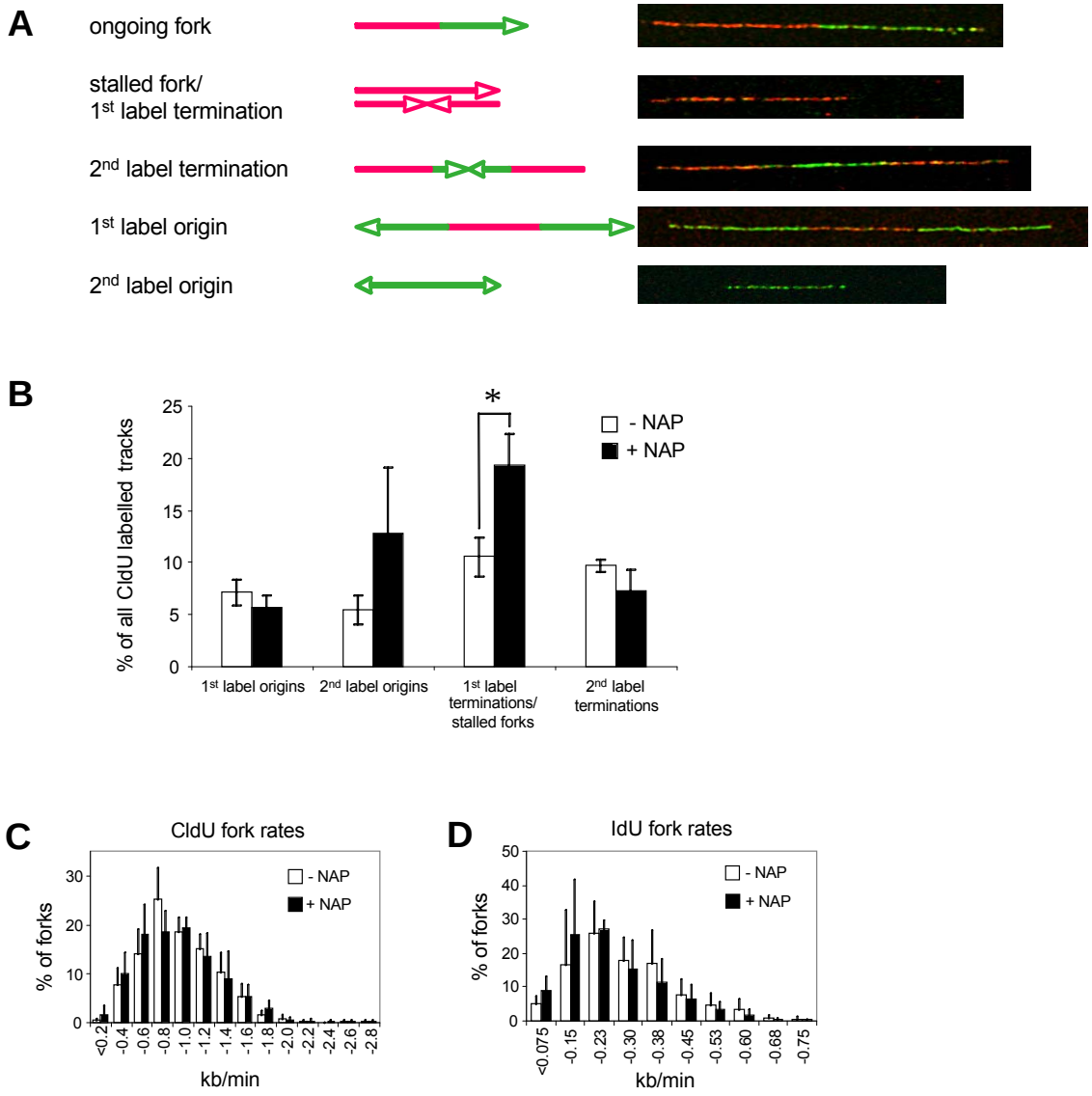

Figure S3. PARP inhibition slows replication elongation and delays restart of replication forks stalled by hydroxyurea treatment. DNA combing analysis of replication forks in U2OS cells pulse pulse labelled with CldU, treated with HU +/- 100μM NAP, and released from HU into IdU +/- 100μM NAP **(A)** Schematics and example images of the different replication structures scored. **(B)** Quantification of replication origins, stalled forks and replication terminations as percentage of all tracks labelled during the first label (CldU). Values marked with asterisks are significantly different (1-tailed student's t-test, p = 0.01). Elevated2nd label origins in PARP-inhibited cells suggest increased origin firing to compensate for the higher fork stalling in those cells. **(C)** Distributions of replication fork rates during the first (CldU) label before HU restart. **(D)** Distribution of replication fork rates during the second (IdU) label after HU restart. Different fork rate scales were used to account for slow replication restart after HU treatment. The means and S.D. (bars) of three independent experiments are shown.

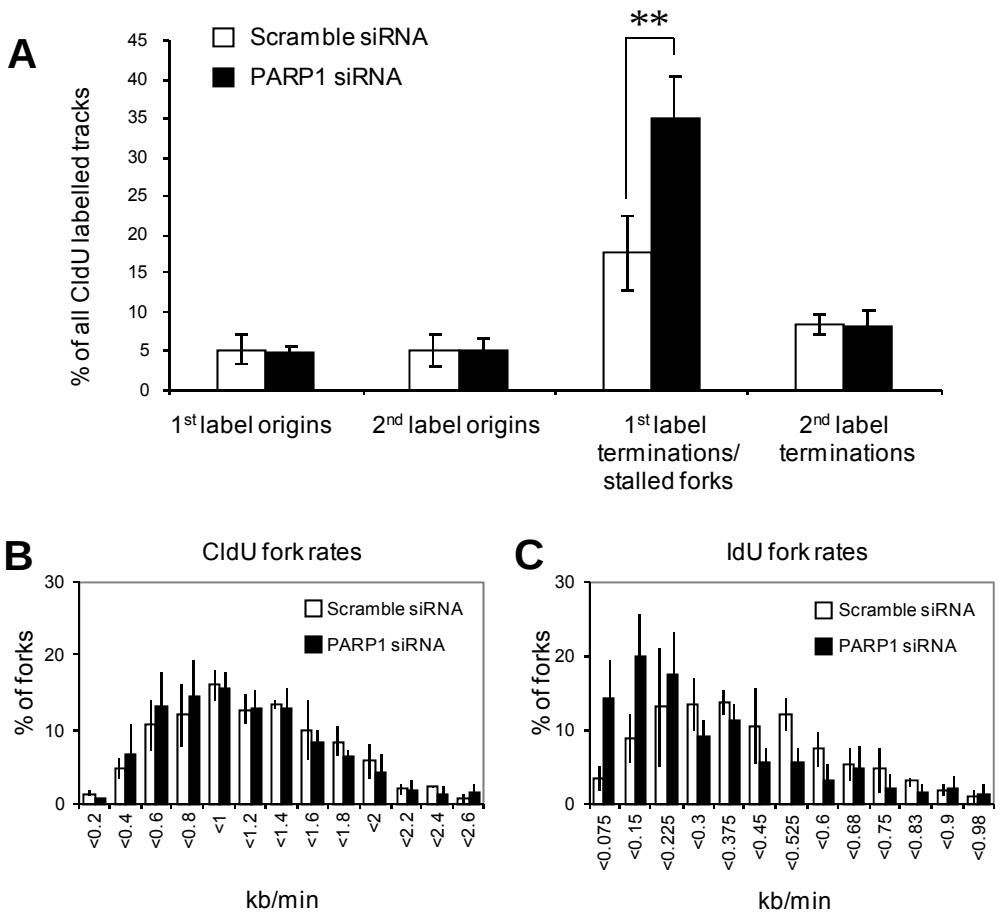

Figure S4. PARP1 siRNA depletion delays restart of replication forks stalled by hydroxyurea treatment. DNA combing analysis of replication fork restart in U2OS cells depleted of PARP1. Cells were labelled to analyse HU restart as in Fig S3. **(A)** Quantification of replication origins, stalled forks and replication terminations as percentage of all tracks labelled during the first label (CldU). Values marked with asterisks are significantly different (1-tailed student's t-test, $p = 0.002$). **(B)** Distributions of replication fork rates during the first (CldU) label before HU restart. **(C)** Distribution of replication fork rates during the second (IdU) label after HU restart. Different fork rate scales were used to account for slow replication restart after HU treatment. Values marked with asterisks are significantly different ($p < 0.02$). The means and S.D. (bars) of three independent experiments are shown.

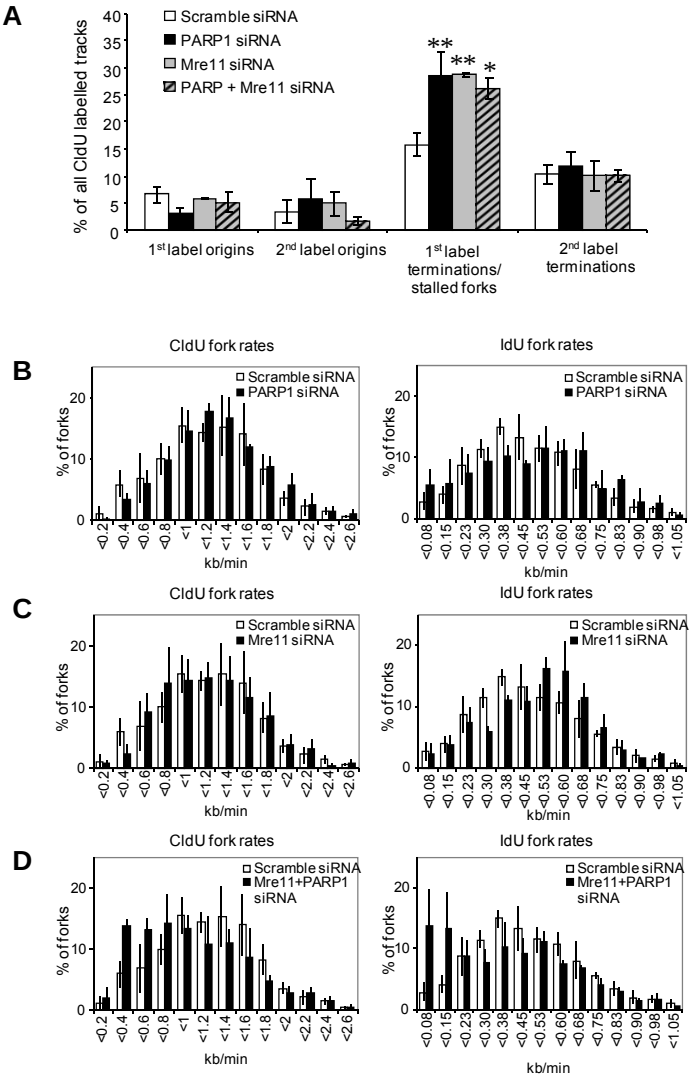

Figure S5. PARP1 and Mre11 siRNA depletion delay replication fork restart by affecting the same pathway. DNA combing analysis of replication fork restart in U2OS cells depleted of PARP1, Mre11, or both. Cells were labelled to analyse HU restart as in Fig S3. **(A)** Quantification of replication origins, stalled forks and replication terminations as percentage of all tracks labelled during the first label (CldU). Values marked with asterisks are significantly different (1-tailed student's t-test, p (scrambled-PARP1) = 0.0016, p (scrambled-Mre11) = 0.008, p (scrambled-PARP1/Mre11) = 0.03). The means and S.D. (bars) of three independent experiments are shown. **(B)-(D)** Distributions of replication fork rates during the first (CldU) label before HU restart and of replication fork rates during the second (IdU) label after HU restart. **(B)** Comparison of Scramble and PARP1 depleted samples. **(C)** Comparison of Scramble and Mre11 depleted samples. **(D)** Comparison of Scramble and PARP1+Mre11 co-depleted samples. Different fork rate scales were used to account for slow replication restart after HU treatment. The means and S.D. (bars) of three independent experiments are shown.

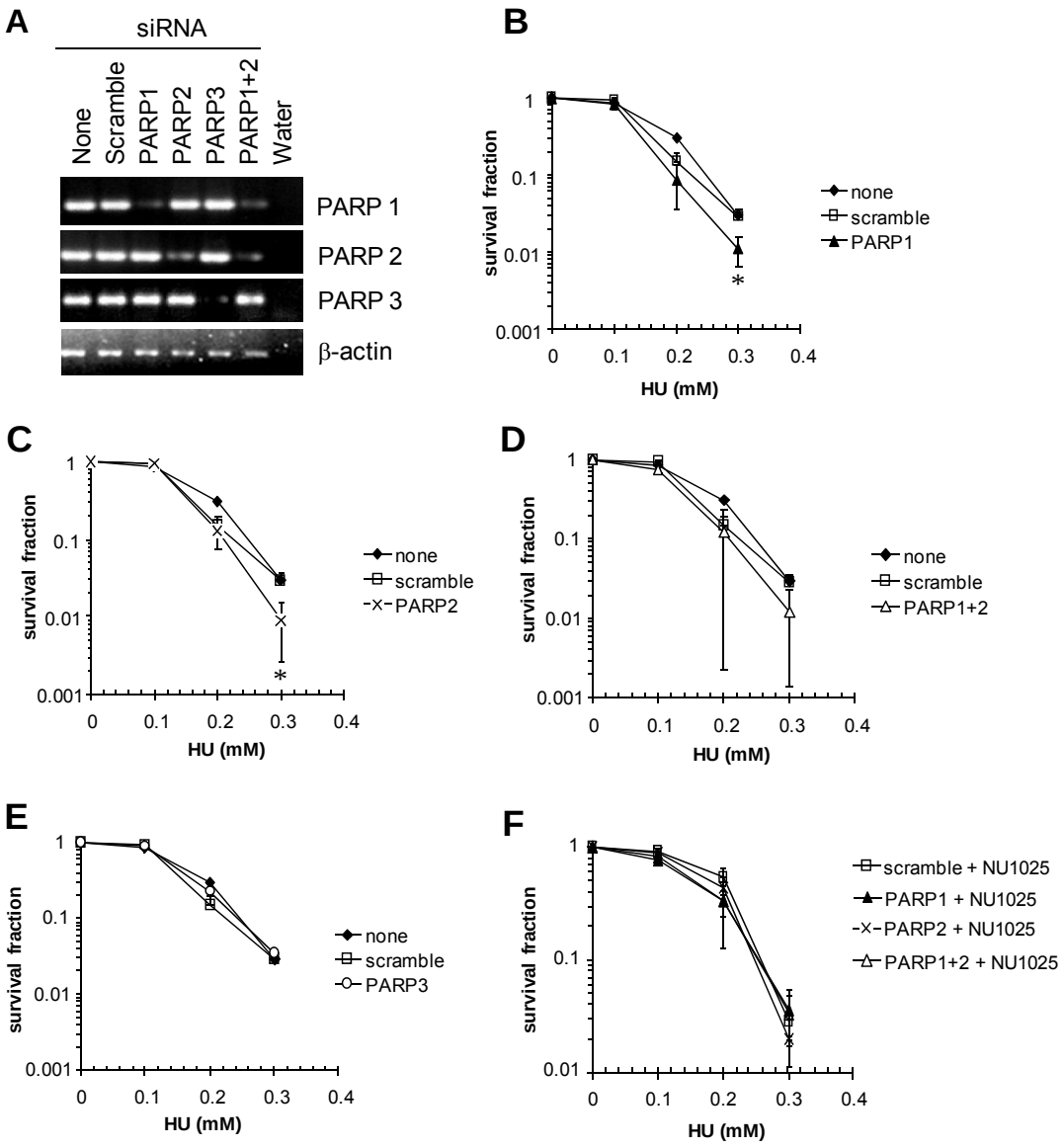

Figure S6 Absence of PARP1 and PARP2 leads to increased sensitivity to hydroxyurea. (A) RT-PCR analysis of mRNAs from SW480SN.3 cells following 48 hours depletion with siRNA. Survival fraction of SW480SN.3 cells depleted of **(B)** PARP1, **(C)** PARP2, **(D)** PARP1+2, **(E)** PARP3, **(F)** PARP1+2 in presence of PARP inhibitor NU1025, following treatment for 24 hours with increasing doses of the replication inhibitor hydroxyurea. The mild sensitivity to hydroxyurea in PARP-depleted cells is likely to be due to incomplete siRNA depletion. The means (symbol) and standard deviations (error bar) from at least three experiments are depicted. Single star indicate significance in t-test $p<0.05$.